Elsevier Editorial System(tm) for
International Journal of Hydrogen Energy
Manuscript Draft

Manuscript Number: HE-D-20-05238R1

Title: Ni alloy nanowires as high efficiency electrode materials for HER in alkaline electrolysers

Article Type: SI: Hypothesis15 (Basile)

Section/Category: Electrolysis / Electrolyzers

Keywords: Alkaline Electrolyzer, Nanostructured Electrodes, Ni-Co Alloy, Ni-W alloy, Ni-Zn alloy, Template Electrosynthesis

Corresponding Author: Professor Rosalinda Inguanta, Prof

Corresponding Author's Institution: Università di Palermo

First Author: Fabrizio Ganci

Order of Authors: Fabrizio Ganci; Bernardo Patella; Giuseppe Aiello; Emanuele Cannata; Valentino Cusumano; Carmelo Sunseri; Philippe Mandin; Rosalinda Inguanta, Prof

Abstract: The fabrication and characterization of nickel-alloy electrodes for alkaline electrolysers is reported. Three different alloys (Ni-Co, Ni-Zn and Ni-W) at different composition were studied in order to determine the optimum solution. Nanostructured electrodes were obtained by template electrodeposition into a nanoporous membrane and starting from aqueous solutions containing the two elements of the alloy at different concentrations. Composition of alloys can be tuned by electrolyte composition and also depends on the difference of the redox potential of elements and on the presence of complexing agents in deposition bath. Electrochemical and electrocatalytic tests aimed at establishing the best alloy composition were carried out for hydrogen evolution reaction. Then, test conducted at a constant current density in potassium hydroxide (30% w/w) aqueous solution were also performed. For all investigated alloys, very encouraging results were obtained and in particular Ni-Co alloys richer in Co showed the best performance.

Dear Editor,

I am sending the revised form of the paper "Ni alloy nanowires as high efficiency electrode materials for alkaline electrolysers" by Fabrizio Ganci et al., which we have submitted for publication as research paper in the HYPOTHESIS XV Special Issue of the International Journal of Hydrogen Energy.

We have taken into consideration the reviewer's suggestions and we responded him in the rebuttal letter. The paper has been modified consequently. Furthermore, as suggested by the Editor, we have improved the literature survey. Therefore, we believe that in the present form the manuscript should be suitable for publication in International Journal of Hydrogen Energy.

We confirm that this manuscript has not been published elsewhere and is not under consideration by another journal. All authors have approved the revised version of manuscript.

With my best regards

Rosalinda Inguanta

Corresponding author:
Dr. Rosalinda Inguanta
Laboratorio Chimica Fisica Applicata
Dipartimento di Ingegneria, Università degli Studi di Palermo, Viale delle Scienze ed. 6, 90128 Palermo, Italy

***Detailed Response to Reviewers**

Click here to download Detailed Response to Reviewers: ResponseToReviewer#1.docx

Reviewer #1:

In the current manuscript the authors investigate The fabrication and characterization of nickel-alloy electrodes for alkaline electrolysers
In my opinion the manuscript could be published in the International Journal of Hydrogen Energy only after the following observations will be taken into consideration:

1)Why authors chosen Cobalt? Cobalt is a critical raw material. Please is needed to justify this on the objective of the paper. Which is the novelty?

Response: As detailed in the revised text, the choice to test cobalt-based electrocatalysts is almost inevitable. Ni-Co alloys showed good performance not just as HER electrocatalyst but also in other fields due to its good magnetic, mechanical and electrical properties. In general, the cobalt-based electrocatalysts have low cell voltage, exclusive electronic structures, and significant durability, this makes them unique for energy-related fields applications. Some references were added in the revised text to support as above reported.

2) The authors have done the TEM analysis? Is it possible report the TEM analysis and table composition EDS, XRD, TEM of materials?

Response: Unfortunately, we cannot do TEM analysis at this time. According to reviewer's suggestion in the revised manuscript we have inserted in the main test Table 3, where the data of Figures 2 and 3 were summarized, while in the Supplementary Material we have inserted Table S1, reporting the identification of peaks of XRD patterns of Figure 4.

3) Concerning Fig. 2,3 and 4 would be better insert a table to comparison the differences and improve the work.

Response: According to reviewer's suggestion in the revised manuscript we have inserted in the main test Table 3, where the data of Figures 2 and 3 were summarized, while in the Supplementary Material we have inserted Table S1, reporting the identification of peaks of XRD patterns of Figure 4.

4) Fig 4 is needed replacement, the diffractogram presents low quality and would be better insert the card number of standards.

Response: According to reviewer's suggestion in the revised manuscript we have modified Figure 4.

5)Can authors insert the galvanostatic polarizations curves?

Response: The galvanostatic polarization curves were reported in Figure 8a of the main text and in Figure 6 of Supplementary Material.

6) A table containing a comparison of HER performance of materials would be appreciate.

Response: According to reviewer's suggestion in the revised text we have added a new Table (Table 4), where the most recent results on the electrocatalytic performance of different materials for alkaline electrolyzes have been reported. In Table 4 our results were also reassumed in order to compare them with the more relevant literature data

7) Comparison of ECSA-normalized activity of different catalysts is needed.

Response: In our previous works, cited in the text, we have esteemed the electrochemical active surface area (ECSA) of the nanostructured electrodes. To avoid to repeat equal results, in this work we have not repeated the same experiments. In particular, we have measured the current density during CV, performed at the same scan and in the same potential range, and we have observed that for a planar electrode of Ni, there is a significant difference in the value, that is lower than recorded for both the NWs of Ni and its alloy. This difference in current densities is

attributable to the difference in electrochemically active surface area between the planar Ni electrode and the nanostructures. Using the current density values, we estimated that the real surface area of the NW electrodes (we have tested NWs with the almost same length) is about two orders of magnitude higher than the planar electrode.
As reported by Anantharaj et al (DOI: 10.1039/C7EE03457A) different methods can be used to determinate the ECSA leading to different values for the same material. This is due to the fact that each electrocatalyst, even if made with the same material, is basically distinguishable by size, shape, morphology, topography and porous nature. Considering these difficulties in determining the correct ECSA value, it is preferable to express this parameter in terms of normalized ECSA activity, which is the approach we have followed, normalizing the current density of nanostructured electrode respect to that measured for a Ni planar electrode. In any case, as underlined by Anantharaj et al, the use of normalized activity ECSA cannot be recommended as an essential activity parameter, because too imprecise and excessively depending of the calculation method.

8)It is suggested the results to be compared with standard material.
Response: The most common material used in the alkaline electrolyzes is Ni, and thus in Table 4 we have reported for comparison the electrocatalytic values relative to Ni planar electrode.

9) The graphical abstract is confusig, please explain better.
Response: According to reviewer's suggestion, Graphical abstract was modified.

***Detailed Response to Reviewers**

Click here to download Detailed Response to Reviewers: ResponseToReviewer#2.docx

Reviewer #2: In their manuscript Ni alloy nanowires as high efficiency electrode materials for HER in alkaline electrolysers, the authors describe the preparation of sets of Ni-alloy nanowires and then their subsequent testing for the HER.
Overall the manuscript is clear and logically structured which makes it easy to follow the arguments of the authors. The work described is also of enouhg novelty to warrant publication in the International Journal of Hydrogen Energy.

Resposnse: We thanks the reviewer for the positive comment.

Response to Editor

Editor's Comment: Additionally your literature survey needs improvement; please expand it. Additional related papers can be found in the International Journal of Hydrogen Energy (IJHE), as well as in other energy and fuel cells related publications.

Response: According to Editor's suggestion in the revised text the literature survey has been improved. In particular, we have added a new Table (Table 4), where the most recent results on the electrocatalytic performance of different materials for alkaline electrolyzes have been reported. In Table 4 our results were also reassumed in order to compare them with the more relevant literature data

Ni alloy nanowires as high efficiency electrode materials for alkaline electrolysers

Fabrizio Ganci[1], Bernardo Patella[1], Emanuele Cannata[1], Valentino Cusumano[1], Giuseppe Aiello[1], Carmelo Sunseri[1], Philippe Mandin[2], Rosalinda Inguanta[1,*1]

[1]Dipartimento di Ingegneria, Università di Palermo, Viale delle Scienze, 90128 Palermo, Italy

[2]Université Bretagne Sud, IRDL UMR CNRS 6027, 56100 Lorient, France

Graphical Abstract

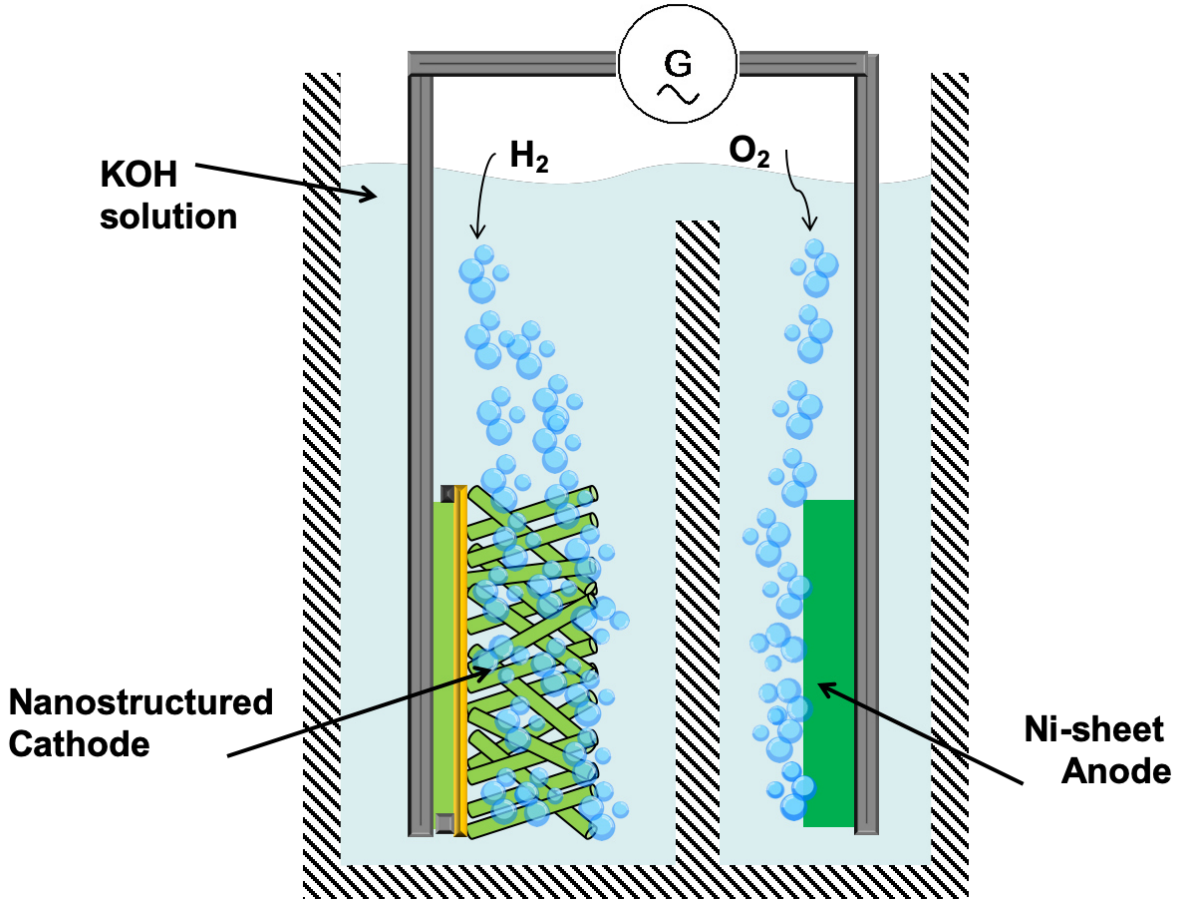

* Corresponding Author: R. Inguanta, Università di Palermo, rosalinda.inguanta@unipa.it

Ni alloy nanowires as high efficiency electrode materials for HER in alkaline electrolysers

Fabrizio Ganci[1], Bernardo Patella[1], Giuseppe Aiello[1], Emanuele Cannata[1], Valentino Cusumano[1], Carmelo Sunseri[1], Philippe Mandin[2], Rosalinda Inguanta[1,*]

[1]Dipartimento di Ingegneria, Università di Palermo, Viale delle Scienze, 90128 Palermo, Italy

[2]Université Bretagne Sud, IRDL UMR CNRS 6027, 56100 Lorient, France

ABSTRACT

The fabrication and characterization of nickel-alloy electrodes for alkaline electrolysers is reported. Three different alloys (Ni-Co, Ni-Zn and Ni-W) at different composition were studied in order to determine the optimum solution. Nanostructured electrodes were obtained by template electrodeposition into a nanoporous membrane and starting from aqueous solutions containing the two elements of the alloy at different concentrations. Composition of alloys can be tuned by electrolyte composition and also depends on the difference of the redox potential of elements and on the presence of complexing agents in deposition bath. Electrochemical and electrocatalytic tests aimed at establishing the best alloy composition were carried out for hydrogen evolution reaction. Then, test conducted at a constant current density in potassium hydroxide (30% w/w) aqueous solution were also performed. For all investigated alloys, very encouraging results were obtained and in particular Ni-Co alloys richer in Co showed the best performance.

KEYWORDS: Alkaline Electrolyzer, Nanostructured Electrodes, Ni-Co Alloy, Ni-W alloy, Ni-Zn alloy, Template Electrosynthesis.

* Corresponding Author: R. Inguanta, Università di Palermo, rosalinda.inguanta@unipa.it

1 INTRODUCTION

Hydrogen production by water electrolysis (WE) is a very promising technology because it is a pollution-free process especially if renewable sources are employed for generating the required energy [1–5]. Although historically it was the first method used for the production of hydrogen, nowadays, the cost of hydrogen production by WE is higher than other available technologies, which makes WE not competitive [6,7]. Despite this, electrolysis is still widely used for the production of hydrogen with a very high degree of purity [8,9]. In particular, today, alkaline electrolysers are the most spread systems in industrial applications [10,11], where the technological maturity ensures good stability and a long lifecycles (over 15 years), as well as high efficiencies (45–85%), and a purity degree of 99.7–99.9% [12,13].

Although alkaline electrolyser is a mature technology, many efforts are still being made to improve its performances and reduce the production costs, through the use of low cost electrodes made of noble-metal-free electrocatalysts [14–18]. In particular, the development of cheap nickel electrodes with high electrocatalytic features is one of the potential approaches to increase the WE performance [19–22]. In the improvement and optimization of the electrode material, of fundamental importance is the morphology of the electrodes which, to ensure high performance, must have very large surface areas [23,24]. For this reason, over the years different types of nanostructured electrodes, which guarantee high aspect ratios, have been developed with 1D [25], 2D [26,27] and 3D morphology [28]. For example, it was demonstrated that $NiFe_2O_4$/carbon black nanospheres have improved catalytic properties towards the electrocatalytic hydrogen evolution reaction (HER) in acidic media [29]. Interesting results were also obtained by Zhang et al., that proposed a P doped nickel-based honeycomb electrode with micro-tapered holes [30]. In particular, they showed that this low-cost and high-efficiency electrocatalyst has superior performances because, at a current

density of 10 $mAcm^{-2}$, requires an overpotential of only 84 mV for the HER. Among the different nanostructured morphologies, nanowires (NWs) are extremely interesting for the development of electrodes for HER reaction [28,31,32]. In particular, as reported by Yan et al. [28], well-ordered NW arrays are ideal to make electrodes for gas evolution because they decrease the pathway of ionic diffusion, enable the ionic motion towards electrode inner part, improve the electrode material utilization degree and favour a rapid release of the gas bubble. Recently, Wang et al. [33] have proposed self-supported Ni-Mo nitride NW arrays that exhibit excellent catalytic activities. In fact, at a current density of 10 $mAcm^{-2}$, for the HER they have measured an overpotentials of 22 mV. Also Li et al. have shown that vertically-aligned Co-Ni-P ternary NW arrays, supported on a nickel foam current collector, have good long-term stability and excellent electrocatalytic performance, attributed to the intrinsically high catalytic activity of ternary alloy and to NWs morphology [34]. Such properties have also been observed by other authors [33], who pointed out that the unique NWs morphology provides a large number of electrocatalytically active sites, offers efficient conductive paths, facilitates the electrolyte mass transport and the release of gas bubbles. Very interesting properties have core-shell Ag/$Ni(OH)_2$ NWs that shows superior activity, high conductivity and good durability [35].

A straightforward method for obtaining electrodes based on ordered arrays of NWs is template electrosynthesis. Through this method, we have fabricated electrodes based on Ni NWs that have a very high surface area and good catalytic performance [36–38]. Besides, we have also shown that Ni NWs obtained by template electrosynthesis and covered with nanoparticles of IrO_2 [19] as an anode and Pd as a cathode [39] of alkaline electrolysers, have good and stable performance also at room temperature.

Here, the attention has been focused on the fabrication and characterization of nickel-alloy electrodes for the HER. In particular, different alloys (Ni-Co, Ni-Zn and Ni-W) with different

composition were studied in order to determine the most suitable alloy and its optimum composition. These alloys were selected due to their promising properties. In particular, as reported in the literature [40], for the HER the expected trend for the activity of alloys should be Ni-Zn > Ni-Co > Ni-W. Besides, the alloys exhibit improved activity compared to pure components as demonstrated by Hong et al. in the case of Ni-Co alloys [41], Sheela et al. for Ni-Zn alloys [42], and by Kim et al. for Ni-W alloys [43]. The superior performance of Ni alloys in comparison with pure elements, were attributed to their unique electronic configuration, characterized by a high number of *d* electrons, that ensures high corrosion resistance, high number of active sites and good electrochemical activity [11,44]. More than the others, Ni-Co alloys showed good performance not just as HER electrocatalyst but also in other fields due to its good magnetic, mechanical and electrical properties [45,46]. In general, the cobalt-based electrocatalysts have low cell voltage, exclusive electronic structures, and significant durability, this makes them unique for energy-related fields applications [47].

In this work, NWs of Ni alloys were obtained by template electrosynthesis using polycarbonate membrane and their performances were evaluated at room temperature using a 30% w/w KOH aqueous solution. Deposition solutions with various concentrations of the two components were used to obtain alloys with different compositions. NWs electrodes of pure Ni, Co and Zn were also fabricated and characterized, to a better comparison between the alloys and to evaluate effective improvement in their use. Only pure metal W NWs was not possible to obtain. To estimate the performances of NW alloys for HER in alkaline medium, electrochemical and electrocatalytic characterization were carried out. In addition, in order to study the mid-term stability of the electrolyser, the electrodes were tested at constant current density.

2 MATERIALS AND METHODS

2.1 Electrode fabrication.

NW electrodes were obtained by template electrosynthesis by means of polycarbonate nanoporous membranes (Whatman). The template has a mean pore diameter of 200 nm and a thickness of about 20 μm. In Table 1, the composition and pH of the deposition solution is reported. With these solutions, pure metallic NW arrays were obtained, whereas, to obtain NWs of two-component alloys, electrodeposition baths with different concentration of metal precursor were used. In particular, starting from the solutions composed exclusively of the two metal precursors, electrolytes with variable composition have been obtained by mixing them in different volumes. The composition of the final solutions, employed to obtain the three alloys at different composition, is reported in Table 2.

Table 1 Composition solution and electrodeposition parameters for pure metallic deposit

Metal	Solution composition	pH	Parameters for NWs deposition
Ni	$NiSO_4 \cdot 6H_2O$ 0.571M NH_4Cl 0.561M CHCOONa 0.366 M H_3BO_3 0.243 M	5.3	Potential Square-Wave: -0.35 V /-0.75 V vs. RHE x 50 cycles
Co	$CoSO_4 \cdot 6H_2O$ 1.07 M $CoCl_2$ 0.34 M H_3BO_3 0.727 M	3.0	Potential Square-Wave: -0.08 V /-0.78 V vs. RHE x 90 cycles
Zn	$ZnSO_4 \cdot 7H_2O$ 0.571M NH_4Cl 0.561M CHCOONa 0.366 M H_3BO_3 0.243 M	5.3	Potential Square-Wave: 0.05 V /-0.75 V vs. RHE x 50 cycles
W	$Na_2WO_4 \cdot 2H_2O$ 0.2 M $Na_3C_6H_5O_7 \cdot 2H_2O$ 0.34 M H_3BO_3 0.323 M NH_4Cl 0.675M $C_3H_8O_3$ 20 mL/L	8.0	/

The electrodeposition was carried out at room temperature, using a fresh solution for each experiment. The electrosynthesis of the templates of NW electrodes was performed according to the procedure detailed in [48–52]. In particular, the first process consists in the sputtering of a very thin layer of gold only on one side of the template. On this gold film, a pure metallic layer of Ni was electrodeposited, potentiostatically at -1.5 V vs. SCE for 2.5 h. This step is of fundamental importance because it permits to obtain a thick and uniform metallic layer that acts both as current collector and as mechanical support for nanostructures.

Table 2 Composition solution and electrodeposition parameters for the template electrosynthesis of NWs of different alloys. The name of the alloys corresponds to the content of the two elements in the electrodeposition bath

Alloy	**Solution composition**		**pH** **Complexing agents**		**Upper and Lower limit of Square wave potential** **Cycle numbers**
Ni-Co					
33-67	$NiSO_4 \cdot 6H_2O$ $NiCl_2$ $CoSO_4 \cdot 6H_2O$ $CoCl_2$	0.356 M 0.11 M 0.713 M 0.23 M			
50-50	$NiSO_4 \cdot 6H_2O$ $NiCl_2$ $CoSO_4 \cdot 6H_2O$ $CoCl_2$	0.535 M 0. 17 M 0.535 M 0.17 M	3.0 H_3BO_3	0.727 M	-0.08 V /-0.78 V vs. RHE 90 cycles
67-33	$NiSO_4 \cdot 6H_2O$ $NiCl_2$ $CoSO_4 \cdot 6H_2O$ $CoCl_2$	0.713 M 0. 23 M 0.356 M 0.11 M			
Ni-Zn					
33-67	$NiSO_4 \cdot 6H_2O$ $ZnSO_4 \cdot 7H_2O$	0.190 M 0.381 M	5.3		-0.35 V /-0.75 V vs. RHE 50 cycles
50-50	$NiSO_4 \cdot 6H_2O$ $ZnSO_4 \cdot 7H_2O$	0.285 M 0.285 M	CHCOONa NH_4Cl H_3BO_3	0.366 M 0.561M 0.243 M	
67-33	$NiSO_4 \cdot 6H_2O$ $ZnSO_4 \cdot 7H_2O$	0.381 M 0.190 M			
Ni-W					
33-67	$NiSO_4 \cdot 6H_2O$ $Na_2WO_4 \cdot 2H_2O$	0.067 M 0.133 M	8.0		-0.06 V /-0.86 V vs. RHE
50-50	$NiSO_4 \cdot 6H_2O$	0.1 M	$Na_3C_6H_5O_7 \cdot 2H_2O$	0.34 M	180 cycles

	$Na_2WO_4 \cdot 2H_2O$	0.1 M	H_3BO_3	0.323 M	
67-33	$NiSO_4 \cdot 6H_2O$	0.133 M	NH_4Cl	0.675M	
	$Na_2WO_4 \cdot 2H_2O$	0.067 M	$C_3H_8O_3$	20 mL/L	

NWs were obtained into the template nanochannels by pulse electrodeposition, using the deposition parameters reported in Table 1 for pure NWs and in Table 2 for NWs alloys. In all cases, to avoid the formation of nanotubes due to the secondary HER, a specifically value of lower applied potential was selected. Template electrosynthesis was performed in a standard cell with three electrodes consisting of a Pt mesh as a counter-electrode and a saturated calomel electrode as a reference (0.242 V vs. SHE). The working electrode area was about 11 cm^2.

To obtain a nanostructured electrode with the array well exposed to the KOH solution during the electrocatalytic tests, a final step of template etching is necessary. In particular, polycarbonate was etched in pure dichloromethane at room temperature. To ensure its total removal, this procedure was repeated 4 times using fresh solvent for each step.

2.2 Electrode Characterization.

The NW electrodes were characterized by scanning electron microscopy (SEM), energy dispersive spectroscopy (EDS) and X-ray diffraction (XRD). In particular, the morphology of NWs was studied by FEG-ESEM microscope (model: QUANTA 200 by FEI). Atomic composition was investigated by EDS analyses, that were carried out only on NWs after their detachment from Ni current collector by a tearing-off with a carbon tape (3M electrically conductive adhesive transfer tape). In order to investigate the uniform composition of NWs, different areas were exanimated. A RIGAKU X-ray diffractometer (model: D-MAX 25600 HK) was employed to perform XRD analyses. Analyses were carried out setting the tube voltage and current at 40 kV and 40 mA, respectively. The 2θ range from 30° to 80°

(sampling width of 0.01°, scan speed of 4.00 °/min) was examined using Ni-filtered Cu Kα radiation (λ= 1.54 Å). The phases were identified by comparison with the literature data. Electrochemical characterizations were carried out in 30% w/w KOH aqueous solution using a three electrode cell, where a Ni sheet (with a surface area of about 20 cm^2) was employed as counter-electrode and Hg/HgO (0.1 M NaOH, 0.165 V vs. SHE) as reference. In the following, all the potentials will be referred to the value of the reversible hydrogen electrode (RHE) at the pH of the relative solution referred to. Cyclic voltammetry (CV, measured in the potential range from -0.035 V to 1.265 V vs. RHE with a scan rate of 0.005 Vs^{-1}) and quasi-steady-state polarization (QSSP) were carried out to study the electrochemical performance of the NW electrodes. The potential range of CV was chosen because at the lower and upper limit HER and OER occur, respectively. QSSP curves (scanned potential range 1 V, scan rate of 0.1667 mVs^{-1}) were obtained in the potential range from 0.1 V to -0.9 V vs. RHE. Besides, to evaluate the mid-term stability, NWs electrodes were subjected to constant current density tests. All electrochemical tests were carried out at room temperature using a Cell Test System (Solartron, Mod. 1470 E). Data were recorded by MultiStat Software. Each experiment reported in this work was repeated at last three times.

3 RESULTS AND DISCUSSUION

3.1 Fabrication and Physico-Chemical Characterization.

The deposition of Ni-alloy NWs was done by applying a square wave potential, using the parameters reported in Table 2. For each alloy, by a preliminary investigation, a specific interval of pulse potential was selected. The pulse potential deposition was chosen because the inversion of current polarity ensures the replenish of the double layer. In addition, the inversion of current density polarity is essential in the case of nanostructures deposition to control their

morphology. In fact, due to the inevitable concurrent HER, the accumulation of hydrogen gas inside the template channels can lead to the formation of nanotubes that have a lower mechanical resistance compared to NWs [49]. Thus, the lower value of potential was selected to have a current density slightly above zero, while the higher value was selected in order to avoid an excessive hydrogen evolution.

The typical voltage and current trend are reported in Figure S1. A similar trend was obtained both for pure Ni and for the alloys (independently from alloy composition) with specific features and values of the reordered pulsed current density. It can be observed that there is a slight difference in the initial form of the current transients, especially when the voltage is inverted from the lowest value to the highest value. In particular, for the Ni-W alloy, the presence of a current spike is observed, attributable to the instantaneous evolution of hydrogen.

In the case of the other alloys and for pure Ni NWs, the initial spike is less evident and seems, in terms of intensity, to follow the same trend of the hydrogen overvoltage in pure metals, that for the elements considered is Zn>Ni>Co>W. Therefore, on the Zn and on the W there are respectively the highest and the lowest overvoltage for the development of hydrogen, which justifies the shape of the registered current transients. In any case, the deposition process led to the formation of regular arrays of NWs (Figure 1). In fact, both for the pure Ni and for the alloys, cylindrical NWs, interconnected with each other, were formed whose shape is specular to that of the polycarbonate template. The NWs were deposited over the entire surface of the electrode and appear firmly connected on the current collector. They have an average diameter of the order of 220-250 nm and a length of about 4 μm.

The morphology of the nanostructures is practically identical in all investigated samples. In fact, none particular differences either between the different alloys, or with the same alloy as its composition varies, were observed (see also Figures S2-S3). This is actually an obvious

result, because in the template electrosynthesis method, the morphology of the nanostructures exactly replicates that of the template and does not depend on the type of material being deposited.

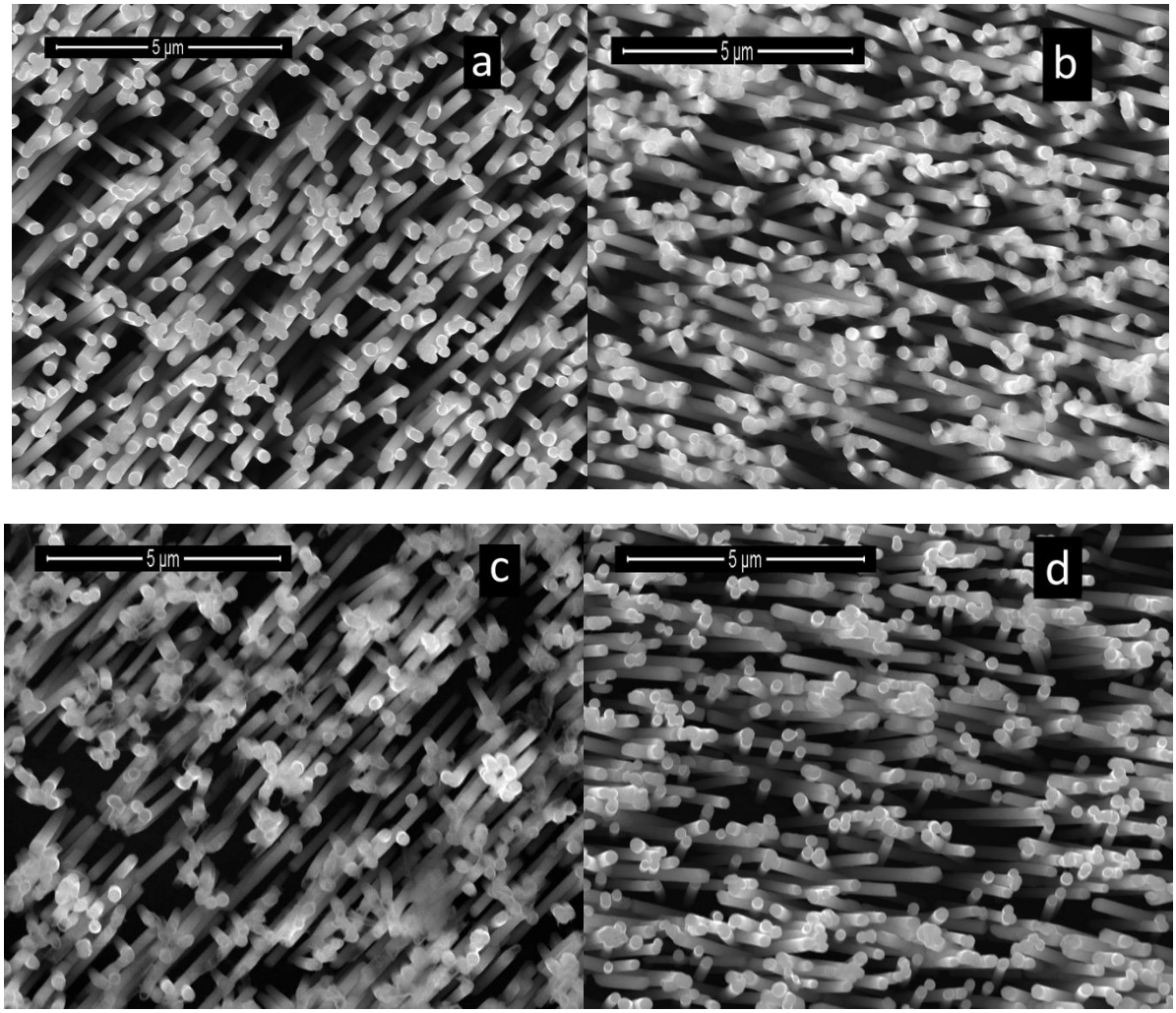

Figure 1. SEM images of Ni and Ni alloy NW electrodes: a) Ni; b) Ni-Co; c) Ni-Zn and d) Ni-W.

Concerning the composition of the nanostructured alloys, the same was determined through EDS measurements that were made on different areas of the sample to verify its homogeneity.

In Figure 2, in particular the EDS spectra of the alloys obtained using an equi-concentration in the electrodeposition bath of the two elements were shown.

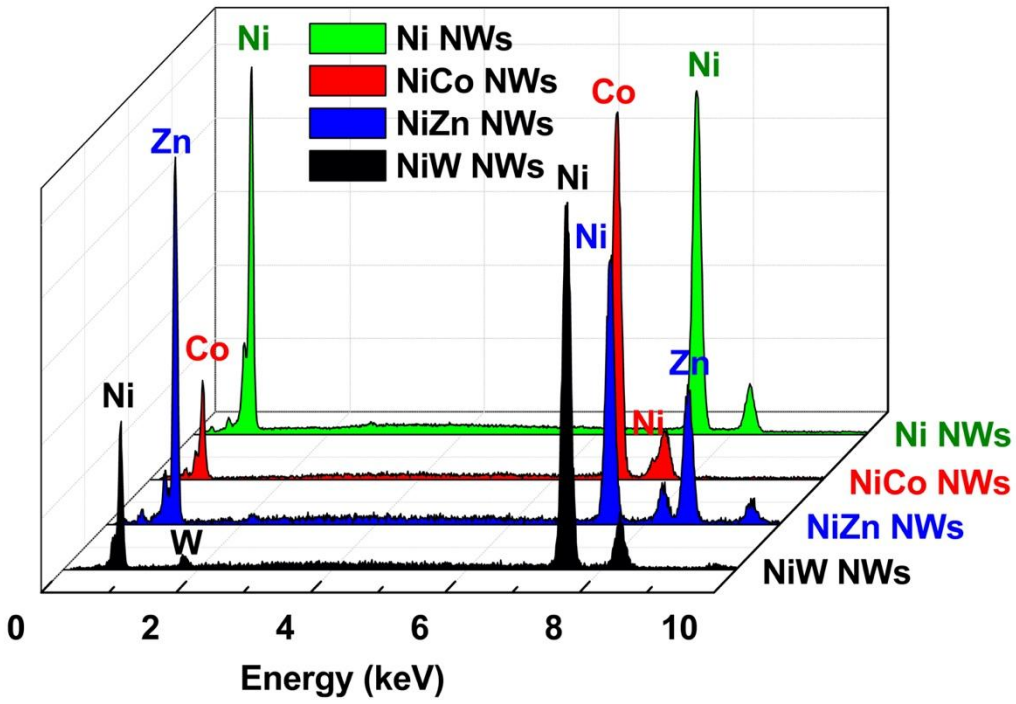

Figure 2. EDS spectra of Ni and Ni alloy NW electrodes: green) Ni; red) Ni-Co; blue) Ni-Zn and black) Ni-W.

As can be observed in Figure 2, apart from the peaks of Ni, and in the case of the alloys, the peaks of the second element that constitutes the alloy itself, no other peaks are present, thus NWs were not contaminated by other elements present in the deposition solution. Therefore, it can be concluded that the NWs are made up of pure Ni and, in the case of the alloys, of a pure alloy. The relative height of the peaks of the two elements changes according to the composition of the bath used for the electrodeposition and this leads to the formation of alloys with different composition (Figure S4). EDS data were summarized in Table 3, where the

NWs atomic composition as a function of element concentration ratio in the electrodeposition solution was reported.

Table 3. NWs atomic composition as a function of element concentration ratio in the electrodeposition solution

Co in Solution (%)	Co in NWs (%)	Zn in Solution (%)	Zn in NWs (%)	W in Solution (%)	W NWs (%)
Ni-Co		Ni-Zn		Ni-W	
0	0	0	0	0	0
5	32.45	16.67	31.03	16.67	0.98
10	47.85	33.33	41.28	33.33	1.55
16.67	66.13	50	44.39	50	2.64
33.33	85.06	66.67	65.51	66.67	2.97
50	92.46	83.33	71.44	83.33	7.48
66.67	94.73	100	100	90	9.15
83.33	97.81				
100	100				

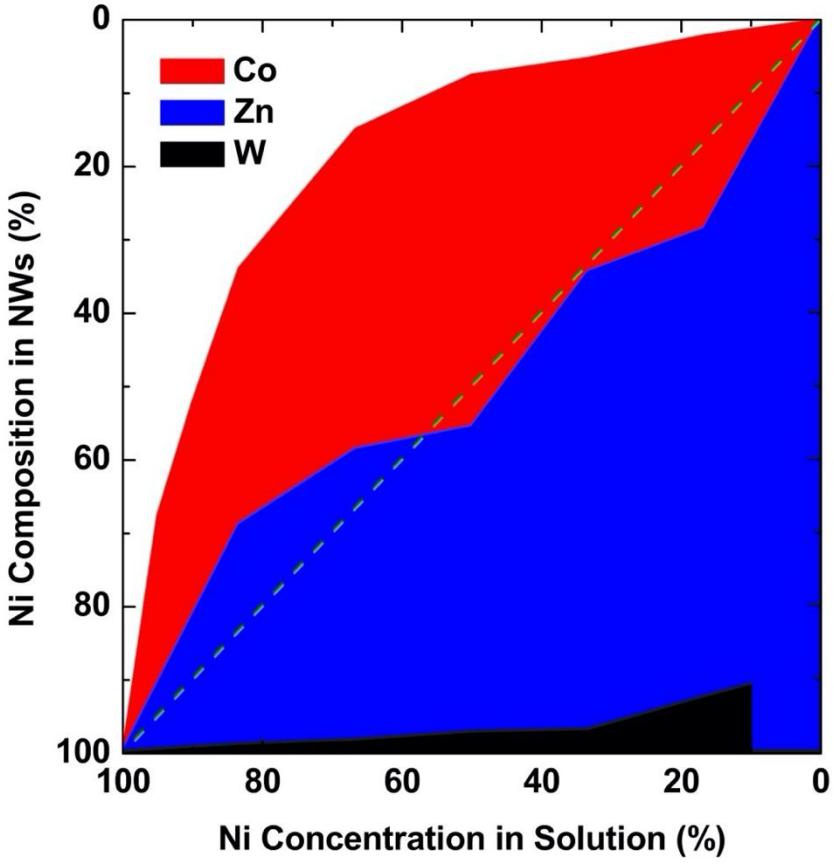

Figure 3. NWs atomic composition as a function of Ni concentration ratio in the electrodeposition solution.

The above discussed is clearly evident in the graph of Figure 3, where the average Ni composition (expressed in atomic %) of the various examined samples as a function of the Ni composition of the electrodeposition bath was reported. In the case of the Ni-Co and Ni-Zn alloys, it was possible to investigate the entire composition interval range, obtaining also the NWs of the pure metals which are obviously representative of the extremes of the composition interval. In the case of the Ni-W alloy, as expected it was not possible to obtain NWs of pure W from an aqueous solution [53]. Despite the presence of a high amount of the W precursor in the electrodeposition bath (Table 2), the alloy with the maximum content of W contained only 10% of its (in the bath the W precursor was 90 %). This is in agreement with the literature data, which shows that for alloys obtained at room temperature (deposition condition also in this work) the maximum solubility of W in Ni is 12.5% [54–56]. In fact, as reported by several authors [43,56–58], the composition of the Ni-W alloy obtained by electrodeposition is little influenced by the composition of the deposition bath and also the current density and the deposition potential have little impact. In the case of the potential, it has also been proved that, for values more cathodic of -0.543 V vs. RHE, due to the concomitant hydrogen development reaction, the amount of deposit that is formed is very small [56]. The only parameter that has an influence on the composition of the Ni-W alloy is the deposition temperature, and in fact Detor et al. [55] have shown that at T higher than room temperature it is possible to obtain alloys with a W content of about 25.5%. Moreover, the same authors have shown that if the alloy deposition occurs through pulse electroplating, a better uniformity of composition is obtained, coherently with what has been obtained and demonstrated here through the EDS measurements of the different areas that have showed the homogeneity of the different samples. The Ni-W alloys reported here were obtained using the classic bath for the electrodeposition of the Ni-W alloy in which the citric-ammonia complex is present (in particular sodium citrate as a complexing agent for Ni and ammonium chloride

for W, respectively). We also added boric acid, considering the results obtained by Wu et al. [59], who reported the formation of a Ni-W alloy at 46% in W thanks to the presence of boric acid in solution. Despite the addition of boric acid, in our deposition conditions, it was not possible to reach such high values of W in the alloy in accordance with what reported by Brenner et al. [60] that have found no influence of this additive on the composition of the alloy.

In the case of the Ni-Zn NWs, the composition of the alloys is approximately linear with the composition of the bath. Considering that the standard electrochemical redox potentials of the two metals are quite different (Ni_{2+}/Ni is 0.04 V vs. RHE, while for Zn^{2+}/Zn is -0.45 V vs. RHE), these results appeared quite surprising. In fact, the thermodynamic values of redox potential suggest an easier deposition of Ni compared to Zn, but this is no longer true in the presence of complexing agents. In fact, our deposition bath contains ammonium chloride and sodium acetate as complexing agents that are known as good additives that improve the Zn electrodeposition rate [42,61–63]. The formation of the alloys, with an almost linear content of Zn, occurs thanks to their presence, which, depending on the composition of the electrolyte, are able to balance the driving force for the deposition of the two components of the alloy.

The composition of Ni-Co alloys appears very complex. In fact, it can be observed that the Co content is higher in the alloy than in the electrolyte, although the very close value of the standard electrochemical potential of Ni^{2+}/Ni (-0.08 V vs. RHE) and Co^{2+}/Co (−0.1 V vs. RHE) would have suggested the formation of an alloy with a composition very similar to that of the bath. These results agree with literature data [45,64], and can be attributable to the specific ligand role of the boric acid in solution towards Ni ions [65]. In fact, considering that the stability constant of Ni-borate complex is higher than Co-Borate one [66], in a

electrodeposition bath containing both, the reduction of Ni^{2+} becomes less favoured leading to a Co enrichment of the alloy.

The XRD patterns of the different nanostructured Ni alloys were showed in Figure 4, where for comparison also the pattern of pure Ni NWs was also reported. These NWs consist of well crystalline α-Ni with face-centered cubic (fcc) structure (ICDD® (International centre of diffraction data) card no. 04-850). The unknown peak at about 40° can be attributable to native oxide of Ni. It can be also observed the peak at 38.7° attributable to the main diffraction point of the metallic gold due to the presence of the sputtered gold film (ICDD® card no. 04-784). As far as the alloys are concerned, the patterns reported in Figure 4 are relative to samples obtained using a bath containing an equi-concentration of the two elements.

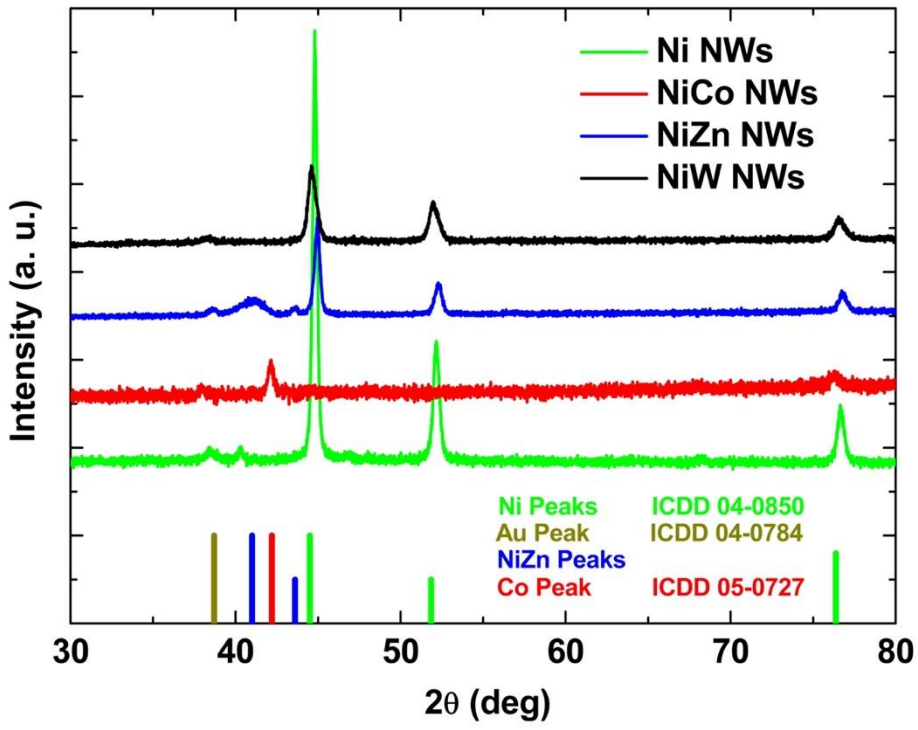

Figure 4. XRD patterns of Ni and Ni alloy NW electrodes: green) Ni; red) Ni-Co; blue) Ni-Zn and black) Ni-W.

For all alloys, it can be observed that the relative intensity of the Ni peaks is very slow compared to that of pure Ni. This, together with the fact that the peaks in the case of alloys are also broader, is attributable to the formation of a deposit with a low grade of crystallinity. The consideration above is particularly true in the case of W alloys. In agreement with the literature data, we have found that the presence of W causes the shift of Ni peaks towards lower diffraction angles [54]. This is attributed to the swelling of the Ni crystal lattice due to the insertion of the W atoms which also tend to make the alloy more or less amorphous. In fact, using Scherrer's equation [67] and according to data obtained by Schuh et al. [54], we have calculated the grain size and found an average size of 12.5± 0.15 nm that is lower of the value calculated for Ni NWs (31.3± 0.15 nm). This effect becomes more evident as W content in the alloy increases.

In addition, in the case of Zn alloy electrode, the peak of gold (38.7°) is present. There are two peaks at 41° and 43.6° that, as reported by Petrauskas et al., are attributable to Ni-Zn alloy [68,69], but the alloy is also confirmed by the broadness of the main Ni peak. In this case, due to the presence of Zn in Ni lattice, we have measured a width at half height, to which correspond an average grain size of 16.7± 0.15 nm, of 0.517° in comparison to 0.275° measured for Ni NWs.

In the case of Co alloys, the main peak of ε-Co phase at about 42.2 (hexagonal close-packed hcp, ICDD® no. 05-0727) appears that shifts towards high 2θ values with the decrease of Co/Ni ratio. For the Co alloy of Figure 4, we have calculated an average grain size of 19.2± 0.15 nm. For high Ni content the characteristic peaks of α-Ni also appear, in agreement with the literature [70]. Alloys rich in Co have a low degree of crystallinity, because similar wide peaks with very low intensity, in comparison to that of Ni, were measured. This result was expected because, as reported by Lu et al. [71], the almost amorphous nature is a typical of Co

and its alloys. For greater clarity, the peaks present in the diffractograms with the relative identification of the phases have been listed in Table S1.

Thus, from XRD characterization, it can be concluded that the Ni alloys obtained in this work have almost nanocrystalline nature regardless of the composition and type of the alloys. This could be an advantage in terms of electrocatalytic performance because, as demonstrated in the case of Ni-Co, amorphous alloys have better performance than the crystalline [72].

3.2 Electrochemical Characterization.

The electrocatalytic behaviour of the Ni-alloy nanostructured electrodes was studied by CV, QSSP, and galvanostatic polarization (GP) at room temperature in an aqueous solution of KOH (30% w/w).

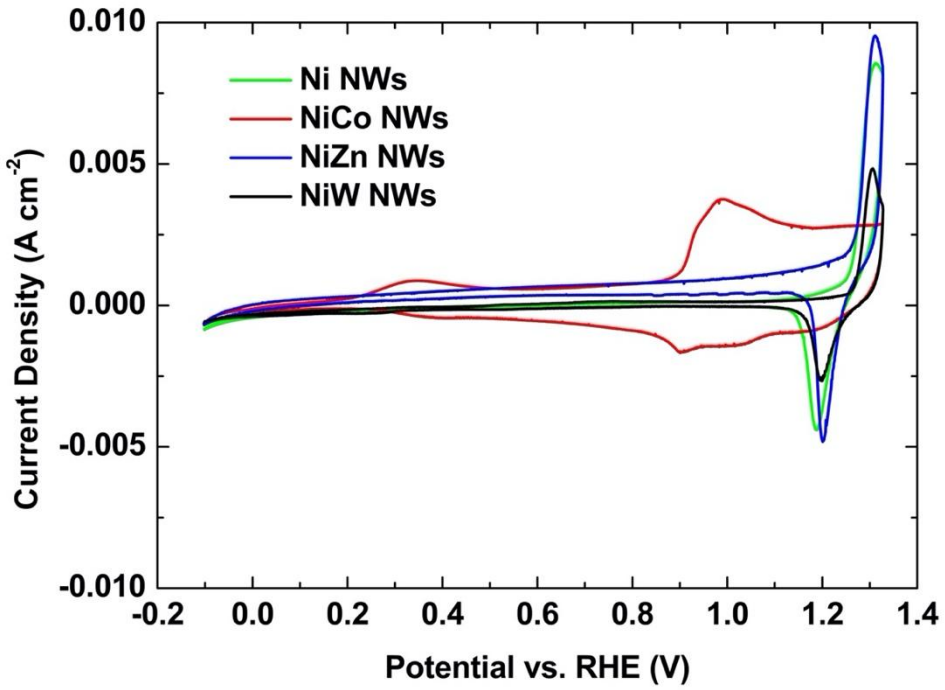

Figure 5. CV curves of Ni and Ni alloy NW electrodes: green) Ni; red) Ni-Co; blue) Ni-Zn and black) Ni-W.

The CV curves of the different alloys, in the potential range from -0.035 V to 1.265 V vs. RHE, are reported in Figure 5 where, for comparison, also the CV of Ni NWs is reported. Also, in this case alloys obtained from a bath containing an equi-concentration of two elements were reported. For Ni NWs in the interval of investigated potential, it is present only a peak in the anodic scan at the potential of about 1.2 V vs. RHE, that, as reported in [73], is attributable to the oxidation of Ni^{2+} to Ni^{3+}. A similar trend was observed for Zn and W alloys, because in the investigated potential range any oxidation-reduction peaks of these alloys are present [42,56]. In the case of Ni-Co alloys, the oxidation peak present in the region between 0.3 and 0.4 V vs. RHE, is due to Co to Co^{2+}. The oxidation and reduction peaks of Co^{2+} / Co^{3+} are also present at 1.00 V vs. RHE and 0.9 V vs. RHE, respectively, according to [74].

The important aspect to underline is that if a CV of a planar electrode of Ni is performed in the same potential range, there is a significant difference in the current density, that is lower than recorded for both the NWs of Ni and its alloys, as demonstrated in our previous article [38]. This difference in current densities is attributable to the difference in electrochemically active surface area (ECSA) between the planar Ni electrode and the nanostructures. Using the current density values, we estimated that the ECSA of the NW electrodes is about two orders of magnitude higher than the planar electrode. As reported by Anantharaj et al [75] this value that we have calculated is only indicative, because different methods can be used to determinate the ECSA leading to different values for the same material. This is due to the fact that each electrocatalyst, even if made with the same material, is typically unique for size, shape, morphology and porous structure.

The QSSP tests were performed in scanned range potential from 0.1 V to -0.9 V vs. RHE with a scan rate of 0.1667 mVs^{-1} in KOH aqueous solution at room temperature. In Figure 6 (see also Figure S5), the only overpotential linear range vs logarithmic current density (reported in absolute value) was reported for alloys obtained from a bath containing an equi-concentration of

two elements. The comparison with Ni NWs allows to observe that the alloying of Ni with different elements is a good strategy to increase its performance. In particular, it can be seen that, at the same overpotential, the highest current density is recorded for the electrode based on Ni-Co alloy, while Ni-Zn and Ni-W NWs seems to have a similar behaviour.

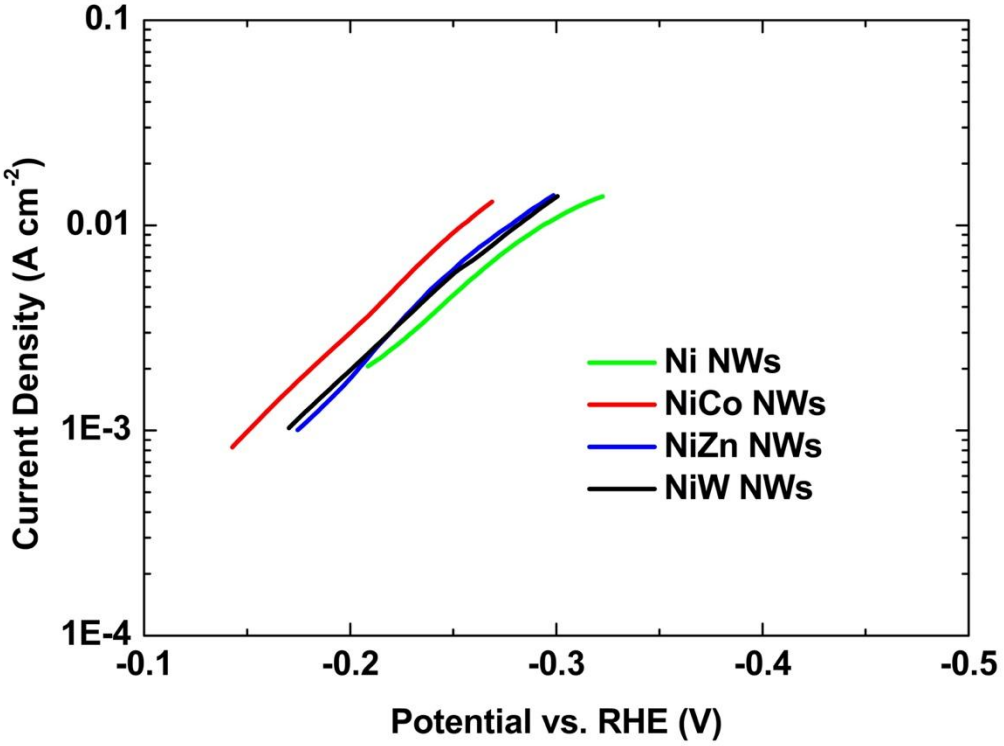

Figure 6. Tafel's curves of Ni and Ni alloy NW electrodes: green) Ni; red) Ni-Co; blue) Ni-Zn and black) Ni-W.

QSSP curves were fitted by Tafel's equation

$$\eta = a + b \log i \qquad (1)$$

Where the a parameter is related to exchanged current density ($a = \frac{-2.303\mathrm{RT}}{\alpha \mathrm{zF}} log i_0$, where z is the electro-chemical equivalent of the reaction and F is the Faraday's constant), while b is the slope of the Tafel's curves. The optimum values of Tafel's slope were reported in Figure 7 (see

also Figure S5 and Table S2). The value of the slope for nanostructured electrode of pure Ni agree with literature data [76]. Besides, as demonstrated in [37] the Tafel's slope value for Ni bare electrode is 0.257 $Vdec^{-1}$, higher than the value calculated for the electrodes here obtained and characterized. This is attributable to the nanostructured morphology that permits to decrease the reaction overpotential. In fact, as reported by Darband et al. [77], electrode with NWs morphology have higher electrocatalytic activity compared to bare ones. This was attributed to the super aerophobic surface of NWs, that guarantees a rapid separation of gas bubbles from the surface [78]. This ensures a high availability of free active sites [79]. For all type of nanostructured alloys here investigated, the Tafel's slope for HER is in the interval between -0.103 $Vdec^{-1}$ and -0.129 $Vdec^{-1}$. Thus, it can be concluded that the Volmer step is the rate determining step [77].

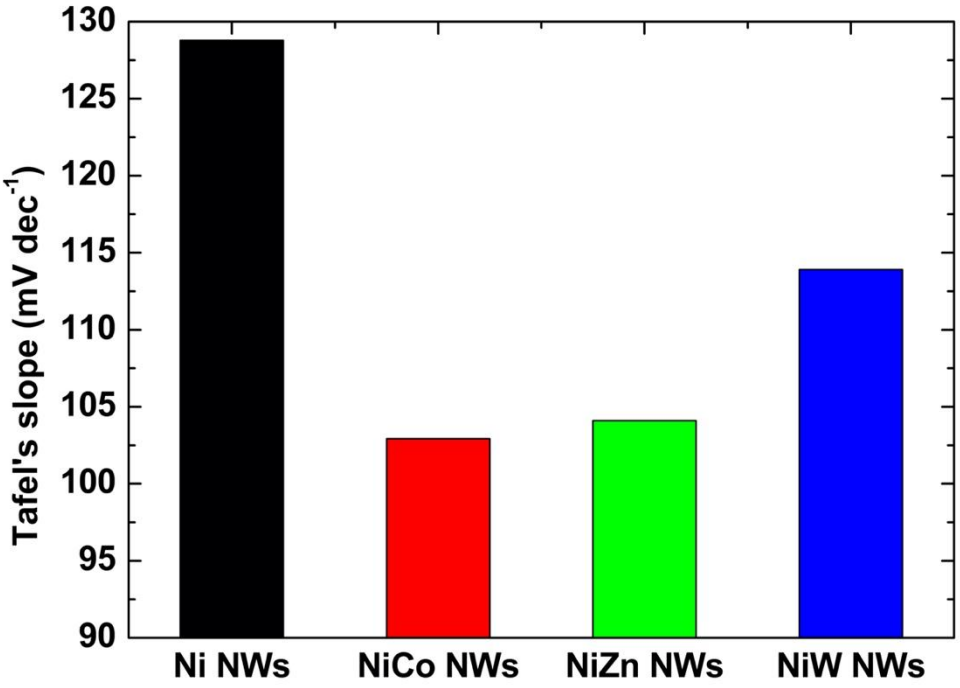

Figure 7. Tafel's slope of Ni and Ni alloy NW electrodes: black) Ni; red) Ni-Co; green) Ni-Zn and blue) Ni-W.

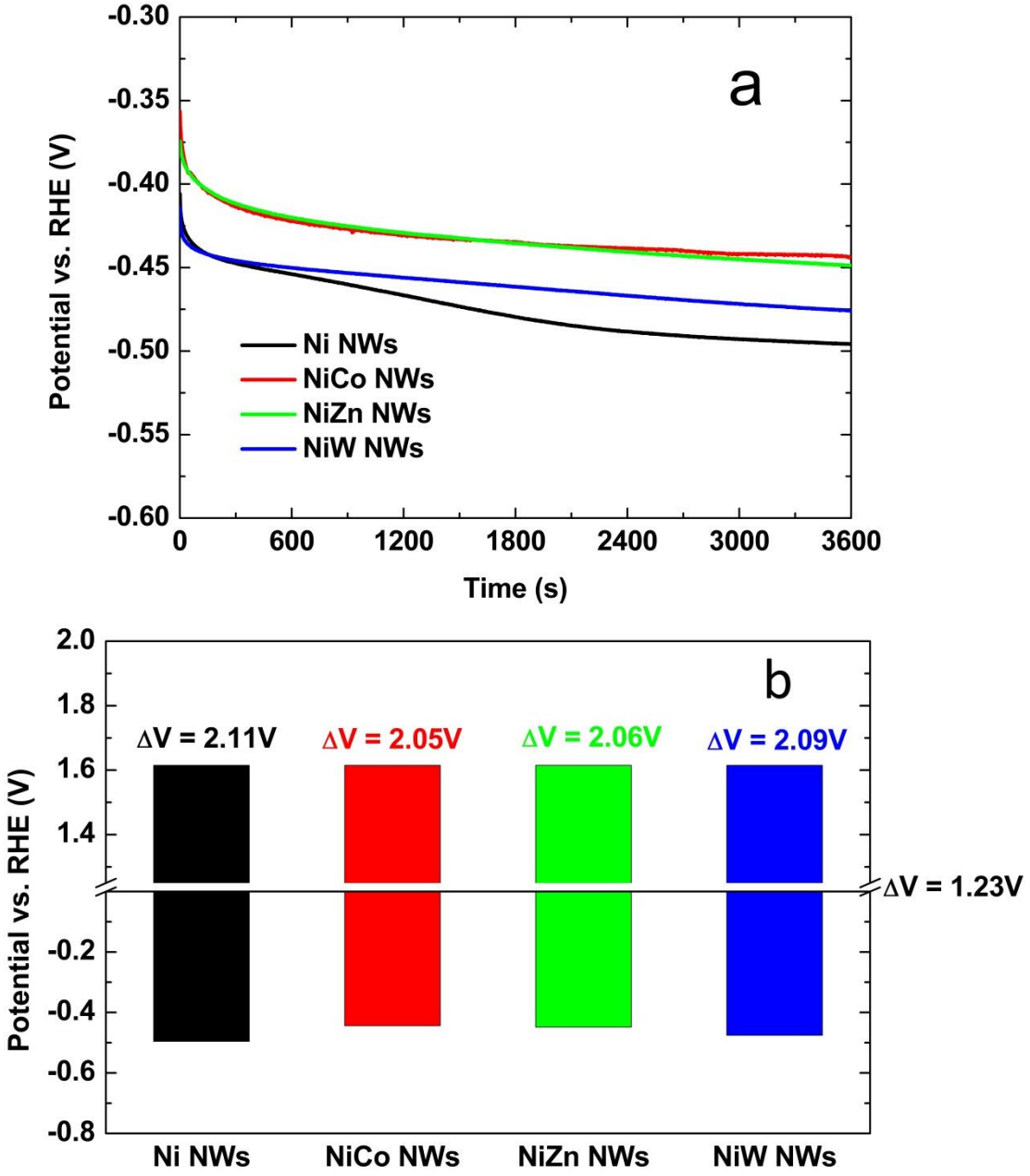

Figure 8. a) Constant current density mid-term stability test and b) mean value of cell potential for Ni and Ni alloy NW electrodes: black) Ni; red) Ni-Co; green) Ni-Zn and blue) Ni-W.

Ni NWs electrodes have the highest slope compared to alloy electrodes. This occurs for all the alloys and for all the compositions (Table S1) investigated. Considering that lower values of Tafel's slope correspond to better electrocatalytic performances of the electrode, it can be concluded that Ni-Co alloys have the best electrocatalytic behaviour for the HER. This behaviour

is attributable both to the high hydrogen adsorption of Co and to the low hydrogen overpotential ensured from Ni [80]. In the case of Zn alloys, the our *b* values are much lower than 0.175 $Vdec^{-1}$ reported by Safizadel et al. [44] for the same type of alloy but not in a nanostructured form. In this case, the best performance was achieved with alloys with a Zn content of about 50%.

For Ni-W nanostructured alloys, b values are similar to those reported in [43]. The improvement of the W alloy, in comparison to pure Ni NWs can be described to the increase of hydrogen absorption due to the amorphous its structure [43].

To evaluate the mid-term behaviour of the nanostructured alloys also galvanostatic tests were performed, using a 30% w/w KOH solution at room temperature and imposing a current density of 0.05 Acm^{-2} for one hour, Figure 8a. the nanostructured alloys used for these tests are those with the best *b* value. During these tests, the cell potential tends to reach an approximately constant value that was reported in Figure 8b (see also Figure S6). In agreement with the above discussed results, the lowest cell voltage was obtained for the Ni-alloy of Co and Zn. Contrarily, in the case of Ni-Co the best performance was found for rich Co alloy, while for Zn alloys the electrodes with the best behaviour is that with a composition of 50% in both elements. We remark the results here discussed were obtained at room temperature, thus the improvement that we have obtained, in comparison to respective planar electrode and others electrode type ~~(see also Table S2, where the performance of some electrodes for HER was listed)~~, can be attributable to the nanostructured morphology that ensures a very high electrochemical active surface area. This suggests that electrodes with NW morphology are possible high-performance cathode for alkaline water electrolysers. In Table 4, the most recent results on the electrocatalytic performance of different materials for HER in alkaline electrolyzes have been reported. From the comparison between the electrodes tested in this work and other electrocatalysts with similar and different chemical composition it can be seen that the Tafel's slope values here obtained are among the lowest to date reported in the literature.

Table 4. Comparison of performance of various electrocatalysts for HER (TW: this work)

Electrocatalysts	KOH solution	Tafel slope (mV/dec)	Current density (mA/cm^2)	Potential at current density (V vs. RHE)	Ref.
Ni strip	30 % w/w	-142			[36]
Ni NWs	30 % w/w	-118	-10	-0.250	[36]
$Ni_{0.95}Ce_{0.05}$	8 M	-126	-10	-0.43	[81]
$Ni_{0.9}Ce_{0.1}$	8 M	-160	-10	-0.466	[81]
NiS_2 HMSs	1 M	-157	-10	-0.219	[82]
NiCo	30 % w/w	-101	-10	-0.234	[83]
p-WP_2	1 M	-131	-10	-0.175	[84]
W-WB_4-WC_x/B_4C	0.1 M	-130	-10	-0.360	[85]
G@Co@Zn@NF-350	1 M	-144	-10	-0.151	[86]
Co_9S_8	1 M NaOH	-110	-10	-0.217	[87]
CoS_x/Ni_3S_2@NF	1 M	-133	-10	-0.204	[88]
$(Ni_{0.33}Co_{0.67})S_2$ NWs/CC	1 M	-127	-10	-0.156	[89]
Co-W/C@NCNSs (600)	1 M	-167	-10	-0.418	[90]
$Co_{50}Ni_{38}Cu_{12}$	6 M	-142	-100	-0.414	[91]
Ni NWs	30 % w/w	-129	-10	-0.295	TW
NiCo NWs 50-50	30 % w/w	-103	-10	-0.257	TW
NiZn NWs 50-50	30 % w/w	-104	-10	-0.276	TW
NiW NWs 50-50	30 % w/w	-114	-10	-0.280	TW

After constant current density mid-term test, SEM analysis of the nanostructured electrodes was performed in order to evaluate the chemical and mechanically stability of the NWs, Figure S7. Compared to as-prepared morphology of the NWs, Figure 1, after the galvanostatic tests there are no particular differences, therefore a chemical stability can be invoked. Furthermore, despite the vigorous development of gases to which the NWs are subject, no detachments, collapses or breakages are evident, indicating their high mechanical stability. This result is very important because it is also an index of the electrochemical stability of the electrodes developed here. A thin patina is present on the top of some of them due to contamination with KOH, formed by precipitation on the electrode after its disassembling from the electrolysis cell and drying in the air as confirmed by EDS analyses that have shown the peak of K (at about 3.3 keV, Figure S8).

CONCLUSION

This study was focused on the performance of nanostructured electrodes as cathodes in alkaline electrolyzer. Specifically, the research concerned different Ni-based metal alloys: the Ni-Co, Ni-Zn and the Ni-W alloy. The obtained nanostructured electrodes, composed of regular arrays of NWs, were manufactured using the simple and inexpensive method of electrodeposition on the template. The advantage of these nanostructures lies in the high active surface on which the electrocatalytic reactions typical of electrochemical cells take place. Ni-W, Ni-Zn, Ni-Co alloy electrodes with different composition were obtained with success by tuning the composition of the electrodeposition bath. The electrodes were subjected to morphological (SEM), chemical-physical (EDS and XRD) and electrochemical (CV, QSSP, and Galvanostatic) characterizations. The results obtained from the electrochemical tests (carried out in a KOH solution at 30% at room temperature) were compared with each other and with the electrode composed of pure nickel in order to select the best electrode. Due to the high surface area, all nanostructured electrodes have showed good performance with respect to planar ones. Besides, a general improvement in alloys performance has been obtained compared to nickel alone.

The best alloy was the one rich in Co, followed by the alloy at 50% in Zn and Ni, while the alloys containing W are characterized only by a slight increase of the performances compared to pure Ni. The nanostructured electrode not only shows a good electrocatalytic activity but also a good chemical and mechanically stability.

More research activities are in progress on the employment of an experimental cell with both nanostructured electrodes, in which it is possible to set temperature, water flow, distance between electrodes, etc.. Furthermore, other activities continue to deal with different

electrocatalysts like Ni-Fe, Ni-Mo or ternary alloys. It is also in progress a study with Ni foam as support to other catalysts

REFERENCES

[1] Imboden C (Hrsg.), Bosnjak D (Hrsg.), Friedrich KA (Hrsg.), Hatziargyriou N (Hrsg.), Kudela T (Hrsg.), Nucci CA (Hrsg.), et al. Proceedings of GSM 2019 2019. https://doi.org/10.5281/ZENODO.3355399.

[2] Cecilia A, Carroquino J, Roda V, Costa-Castelló R, Barreras F. Optimal Energy Management in a Standalone Microgrid, with Photovoltaic Generation, Short-Term Storage, and Hydrogen Production. Energies 2020;13:1454. https://doi.org/10.3390/en13061454.

[3] Carroquino J, Roda V, Mustata R, Yago J, Valiño L, Lozano A, et al. Combined production of electricity and hydrogen from solar energy and its use in the wine sector. Renewable Energy 2018;122:251–63. https://doi.org/10.1016/j.renene.2018.01.106.

[4] Brauns J, Turek T. Alkaline Water Electrolysis Powered by Renewable Energy: A Review. Processes 2020;8:248. https://doi.org/10.3390/pr8020248.

[5] Gandía LM, Oroz R, Ursúa A, Sanchis P, Diéguez PM. Renewable Hydrogen Production: Performance of an Alkaline Water Electrolyzer Working under Emulated Wind Conditions. Energy Fuels 2007;21:1699–706. https://doi.org/10.1021/ef060491u.

[6] Guerra OJ, Eichman J, Kurtz J, Hodge B-M. Cost Competitiveness of Electrolytic Hydrogen. Joule 2019;3:2425–43. https://doi.org/10.1016/j.joule.2019.07.006.

[7] Kayfeci M, Keçebaş A, Bayat M. Hydrogen production. Solar Hydrogen Production, Elsevier; 2019, p. 45–83. https://doi.org/10.1016/B978-0-12-814853-2.00003-5.

[8] Coutanceau C, Baranton S, Audichon T. Hydrogen Production From Water Electrolysis. Hydrogen Electrochemical Production, Elsevier; 2018, p. 17–62. https://doi.org/10.1016/B978-0-12-811250-2.00003-0.

[9] Ursua A, Gandia LM, Sanchis P. Hydrogen Production From Water Electrolysis: Current Status and Future Trends. Proc IEEE 2012;100:410–26. https://doi.org/10.1109/JPROC.2011.2156750.

[10] David M, Ocampo-Martínez C, Sánchez-Peña R. Advances in alkaline water electrolyzers: A review. Journal of Energy Storage 2019;23:392–403. https://doi.org/10.1016/j.est.2019.03.001.

[11] Santos DMF, Sequeira CAC, Figueiredo JL. Hydrogen production by alkaline water electrolysis. Quím Nova 2013;36:1176–93. https://doi.org/10.1590/S0100-40422013000800017.

[12] Le Bideau D, Mandin P, Benbouzid M, Kim M, Sellier M, Ganci F, et al. Eulerian Two-Fluid Model of Alkaline Water Electrolysis for Hydrogen Production. Energies 2020;13. https://doi.org/10.3390/en13133394.

[13] Le Bideau D, Mandin P, Benbouzid M, Kim M, Sellier M. Review of necessary thermophysical properties and their sensivities with temperature and electrolyte mass fractions for alkaline water electrolysis multiphysics modelling. International Journal of Hydrogen Energy 2019;44:4553–69. https://doi.org/10.1016/j.ijhydene.2018.12.222.

[14] Eftekhari A. Electrocatalysts for hydrogen evolution reaction. International Journal of Hydrogen Energy 2017;42:11053–77. https://doi.org/10.1016/j.ijhydene.2017.02.125.

[15] School of Mechanical Engineering, Xi'an Technological University, Xian, P.R. China, Han Q. Recent Development of Metal Alloy Nanostructures for Electrochemical Hydrogen Generation. Int J Electrochem Sci 2019:11549–59. https://doi.org/10.20964/2019.12.21.
[16] Vij V, Sultan S, Harzandi AM, Meena A, Tiwari JN, Lee W-G, et al. Nickel-Based Electrocatalysts for Energy-Related Applications: Oxygen Reduction, Oxygen Evolution, and Hydrogen Evolution Reactions. ACS Catal 2017;7:7196–225. https://doi.org/10.1021/acscatal.7b01800.
[17] Colli AN, Girault HH, Battistel A. Non-Precious Electrodes for Practical Alkaline Water Electrolysis. Materials 2019;12:1336. https://doi.org/10.3390/ma12081336.
[18] Sapountzi FM, Gracia JM, Weststrate CJ (Kees-J, Fredriksson HOA, Niemantsverdriet JW (Hans). Electrocatalysts for the generation of hydrogen, oxygen and synthesis gas. Progress in Energy and Combustion Science 2017;58:1–35. https://doi.org/10.1016/j.pecs.2016.09.001.
[19] Battaglia M, Inguanta R, Piazza S, Sunseri C. Fabrication and characterization of nanostructured Ni–IrO2 electrodes for water electrolysis. International Journal of Hydrogen Energy 2014;39:16797–805. https://doi.org/10.1016/j.ijhydene.2014.08.065.
[20] Razmjooei F, Liu T, Azevedo DA, Hadjixenophontos E, Reissner R, Schiller G, et al. Improving plasma sprayed Raney-type nickel–molybdenum electrodes towards high-performance hydrogen evolution in alkaline medium. Sci Rep 2020;10:10948. https://doi.org/10.1038/s41598-020-67954-y.
[21] Wang L, Weissbach T, Reissner R, Ansar A, Gago AS, Holdcroft S, et al. High Performance Anion Exchange Membrane Electrolysis Using Plasma-Sprayed, Non-Precious-Metal Electrodes. ACS Appl Energy Mater 2019;2:7903–12. https://doi.org/10.1021/acsaem.9b01392.
[22] Khan MA, Zhao H, Zou W, Chen Z, Cao W, Fang J, et al. Recent Progresses in Electrocatalysts for Water Electrolysis. Electrochem Energ Rev 2018;1:483–530. https://doi.org/10.1007/s41918-018-0014-z.
[23] TechConnect World Innovation Conference and Expo. TechConnect briefs 2017. Vol. 2: Materials for energy, efficiency and sustainability. Danville, CA, U.S.A: TechConnect; 2017.
[24] López-Fernández E, Gil-Rostra J, Espinós JP, González-Elipe AR, de Lucas Consuegra A, Yubero F. Chemistry and Electrocatalytic Activity of Nanostructured Nickel Electrodes for Water Electrolysis. ACS Catal 2020;10:6159–70. https://doi.org/10.1021/acscatal.0c00856.
[25] Wei Y, Ren X, Ma H, Sun X, Zhang Y, Kuang X, et al. $CoC_2O_4 \cdot 2H_2O$ derived Co_3O_4 nanorods array: a high-efficiency 1D electrocatalyst for alkaline oxygen evolution reaction. Chem Commun 2018;54:1533–6. https://doi.org/10.1039/C7CC08423D.
[26] Chandrasekaran S, Ma D, Ge Y, Deng L, Bowen C, Roscow J, et al. Electronic structure engineering on two-dimensional (2D) electrocatalytic materials for oxygen reduction, oxygen evolution, and hydrogen evolution reactions. Nano Energy 2020;77:105080. https://doi.org/10.1016/j.nanoen.2020.105080.
[27] Li X, Wang J. One- dimensional and two- dimensional synergized nanostructures for high- performing energy storage and conversion. InfoMat 2020;2:3–32. https://doi.org/10.1002/inf2.12040.
[28] Yan Y, Thia L, Xia BY, Ge X, Liu Z, Fisher A, et al. Construction of Efficient 3D Gas Evolution Electrocatalyst for Hydrogen Evolution: Porous FeP Nanowire Arrays on Graphene Sheets. Adv Sci 2015;2:1500120. https://doi.org/10.1002/advs.201500120.
[29] Munonde TS, Zheng H, Matseke MS, Nomngongo PN, Wang Y, Tsiakaras P. A green approach for enhancing the electrocatalytic activity and stability of NiFe2O4/CB nanospheres

towards hydrogen production. Renewable Energy 2020;154:704–14. https://doi.org/10.1016/j.renene.2020.03.022.
[30] Zhang F, Ji R, Liu Y, Pan Y, Cai B, Li Z, et al. A novel nickel-based honeycomb electrode with microtapered holes and abundant multivacancies for highly efficient overall water splitting. Applied Catalysis B: Environmental 2020;276:119141. https://doi.org/10.1016/j.apcatb.2020.119141.
[31] Li G, Wang X, Seo MH, Hemmati S, Yu A, Chen Z. Design of ultralong single-crystal nanowire-based bifunctional electrodes for efficient oxygen and hydrogen evolution in a mild alkaline electrolyte. J Mater Chem A 2017;5:10895–901. https://doi.org/10.1039/C7TA02745A.
[32] Nairan A, Zou P, Liang C, Liu J, Wu D, Liu P, et al. NiMo Solid Solution Nanowire Array Electrodes for Highly Efficient Hydrogen Evolution Reaction. Adv Funct Mater 2019;29:1903747. https://doi.org/10.1002/adfm.201903747.
[33] Wang Y, Sun Y, Yan F, Zhu C, Gao P, Zhang X, et al. Self-supported NiMo-based nanowire arrays as bifunctional electrocatalysts for full water splitting. J Mater Chem A 2018;6:8479–87. https://doi.org/10.1039/C8TA00517F.
[34] Li W, Xiong D, Gao X, Song W-G, Xia F, Liu L. Self-supported Co-Ni-P ternary nanowire electrodes for highly efficient and stable electrocatalytic hydrogen evolution in acidic solution. Catalysis Today 2017;287:122–9. https://doi.org/10.1016/j.cattod.2016.09.007.
[35] Liu Y, Zhang G, Zuo C, Zhao K, Zeng J, Yin J, et al. Core-Shell AgNWs@Ni(OH) $_2$ Nanowires Anchored on Filter Paper for Efficient Hydrogen Evolution Reaction. J Electrochem Soc 2020;167:116520. https://doi.org/10.1149/1945-7111/aba4e4.
[36] Ganci F, Baguet T, Aiello G, Cusumano V, Mandin P, Sunseri C, et al. Nanostructured Ni Based Anode and Cathode for Alkaline Water Electrolyzers. Energies 2019;12:3669. https://doi.org/10.3390/en12193669.
[37] Ganci F, Cusumano V, Sunseri C, Inguanta R. Performance Enhancement of Alkaline Water Electrolyzer Using Nanostructured Electrodes Synthetized by Template Electrosynthesis. 2018 IEEE 4th International Forum on Research and Technology for Society and Industry (RTSI), Palermo: IEEE; 2018, p. 1–4. https://doi.org/10.1109/RTSI.2018.8548399.
[38] Ganci F, Lombardo S, Sunseri C, Inguanta R. Nanostructured electrodes for hydrogen production in alkaline electrolyzer. Renewable Energy 2018;123:117–24. https://doi.org/10.1016/j.renene.2018.02.033.
[39] Fabrizio Ganci, Rosalinda Inguanta, Salvatore Piazza, Carmelo Sunseri, Salvatore Lombardo. Fabrication and characterization of nanostructured ni and pd electrodes for hydrogen evolution reaction (her) in water-alkaline electrolyzer. Chemical Engineering Transactions 2017;57:1591–6. https://doi.org/10.3303/CET1757266.
[40] Li X, Hao X, Abudula A, Guan G. Nanostructured catalysts for electrochemical water splitting: current state and prospects. J Mater Chem A 2016;4:11973–2000. https://doi.org/10.1039/C6TA02334G.
[41] Hong SH, Ahn SH, Choi I, Pyo SG, Kim H-J, Jang JH, et al. Fabrication and evaluation of nickel cobalt alloy electrocatalysts for alkaline water splitting. Applied Surface Science 2014;307:146–52. https://doi.org/10.1016/j.apsusc.2014.03.197.
[42] Sheela G. Zinc–nickel alloy electrodeposits for water electrolysis. International Journal of Hydrogen Energy 2002;27:627–33. https://doi.org/10.1016/S0360-3199(01)00170-7.

[43] Hong SH, Ahn SH, Choi J, Kim JY, Kim HY, Kim H-J, et al. High-activity electrodeposited NiW catalysts for hydrogen evolution in alkaline water electrolysis. Applied Surface Science 2015;349:629–35. https://doi.org/10.1016/j.apsusc.2015.05.040.
[44] Safizadeh F, Ghali E, Houlachi G. Electrocatalysis developments for hydrogen evolution reaction in alkaline solutions – A Review. International Journal of Hydrogen Energy 2015;40:256–74. https://doi.org/10.1016/j.ijhydene.2014.10.109.
[45] Lupi C, Dell'Era A, Pasquali M. Nickel–cobalt electrodeposited alloys for hydrogen evolution in alkaline media. International Journal of Hydrogen Energy 2009;34:2101–6. https://doi.org/10.1016/j.ijhydene.2009.01.015.
[46] Karimzadeh A, Aliofkhazraei M, Walsh FC. A review of electrodeposited Ni-Co alloy and composite coatings: Microstructure, properties and applications. Surface and Coatings Technology 2019;372:463–98. https://doi.org/10.1016/j.surfcoat.2019.04.079.
[47] Maiti A. Cobalt-based heterogeneous catalysts in an electrolyzer system for sustainable energy storage. Dalton Trans 2020;49:11430–50. https://doi.org/10.1039/D0DT01469A.
[48] Inguanta R, Rinaldo E, Piazza S, Sunseri C. Lead Nanowires for Microaccumulators Obtained Through Indirect Electrochemical Template Deposition. Electrochem Solid-State Lett 2010;13:K1. https://doi.org/10.1149/1.3246944.
[49] Silipigni L, Barreca F, Fazio E, Neri F, Spanò T, Piazza S, et al. Template Electrochemical Growth and Properties of Mo Oxide Nanostructures. J Phys Chem C 2014;118:22299–308. https://doi.org/10.1021/jp505819j.
[50] Battaglia M, Piazza S, Sunseri C, Inguanta R. Amorphous silicon nanotubes via galvanic displacement deposition. Electrochemistry Communications 2013;34:134–7. https://doi.org/10.1016/j.elecom.2013.05.041.
[51] Carmelo Sunseri, Cristina Cocchiara, Fabrizio Ganci, Alessandra Moncada, Roberto Luigi Oliveri, Bernardo Patella, et al. Nanostructured electrochemical devices for sensing, energy conversion and storage. Chemical Engineering Transactions 2016;47:43–8. https://doi.org/10.3303/CET1647008.
[52] Inguanta R, Piazza S, Sunseri C, Cino A, Di Dio V, Cascia DL, et al. An electrochemical route towards the fabrication of nanostructured semiconductor solar cells. SPEEDAM 2010, Pisa, Italy: IEEE; 2010, p. 1166–71. https://doi.org/10.1109/SPEEDAM.2010.5542264.
[53] Schlesinger M, Paunovic M, editors. Modern electroplating. 5th ed. Hoboken, NJ: Wiley; 2010.
[54] Schuh CA, Nieh TG, Iwasaki H. The effect of solid solution W additions on the mechanical properties of nanocrystalline Ni. Acta Materialia 2003;51:431–43. https://doi.org/10.1016/S1359-6454(02)00427-5.
[55] Detor A, Schuh C. Tailoring and patterning the grain size of nanocrystalline alloys. Acta Materialia 2007;55:371–9. https://doi.org/10.1016/j.actamat.2006.08.032.
[56] Obradović MD, Stevanović RM, Despić AR. Electrochemical deposition of Ni–W alloys from ammonia–citrate electrolyte. Journal of Electroanalytical Chemistry 2003;552:185–96. https://doi.org/10.1016/S0022-0728(03)00151-7.
[57] Yamasaki T. HIGH-STRENGTH NANOCRYSTALLINE Ni-W ALLOYS PRODUCED BY ELECTRODEPOSITION n.d.:6.
[58] Younes O, Gileadi E. Electroplating of Ni /W Alloys. J Electrochem Soc 2002;149:C100. https://doi.org/10.1149/1.1433750.
[59] Wu Y, Chang D, Kim D, Kwon S-C. Influence of boric acid on the electrodepositing process and structures of Ni–W alloy coating. Surface and Coatings Technology 2003;173:259–64. https://doi.org/10.1016/S0257-8972(03)00449-3.

[60] Brenner A, Burkhead P, Seegmiller E. Electrodeposition of tungsten alloys containing iron, nickel, and cobalt. J RES NATL BUR STAN 1947;39:351. https://doi.org/10.6028/jres.039.023.
[61] Panzeri G, Muller D, Accogli A, Gibertini E, Mauri E, Rossi F, et al. Zinc electrodeposition from a chloride-free non-aqueous solution based on ethylene glycol and acetate salts. Electrochimica Acta 2019;296:465–72. https://doi.org/10.1016/j.electacta.2018.11.060.
[62] Lotfi N, Aliofkhazraei M, Rahmani H, Darband GhB. Zinc–Nickel Alloy Electrodeposition: Characterization, Properties, Multilayers and Composites. Prot Met Phys Chem Surf 2018;54:1102–40. https://doi.org/10.1134/S2070205118060187.
[63] Zhang J, Zhou Y, Zhang S, Li S, Hu Q, Wang L, et al. Electrochemical Preparation and Post-treatment of Composite Porous Foam NiZn Alloy Electrodes with High Activity for Hydrogen Evolution. Sci Rep 2018;8:15071. https://doi.org/10.1038/s41598-018-33205-4.
[64] Bai A, Hu C-C. Effects of electroplating variables on the composition and morphology of nickel–cobalt deposits plated through means of cyclic voltammetry. Electrochimica Acta 2002;47:3447–56. https://doi.org/10.1016/S0013-4686(02)00281-5.
[65] Graff A, Barrez E, Baranek P, Bachet M, Bénézeth P. Complexation of Nickel Ions by Boric Acid or (Poly)borates. J Solution Chem 2017;46:25–43. https://doi.org/10.1007/s10953-016-0555-x.
[66] Bousher A. REVIEW: UNIDENTATE COMPLEXES INVOLVING BORATE. Journal of Coordination Chemistry 1995;34:1–11. https://doi.org/10.1080/00958979508024298.
[67] West AR. Solid state chemistry and its applications. Second edition, student edition. Chichester, West Sussex, UK: Wiley; 2014.
[68] Petrauskas A, Grincevičienė L, Češūnienė A, Juškėnas R. Study of phase composition of Zn–Ni alloy electrodeposited in acetate–chloride electrolyte at a temperature of 50°C. Electrochimica Acta 2006;51:4204–9. https://doi.org/10.1016/j.electacta.2005.11.040.
[69] Petrauskas A, Grincevičienė L, Češūnienė A, Juškėnas R. Studies of phase composition of Zn–Ni alloy obtained in acetate-chloride electrolyte by using XRD and potentiodynamic stripping. Electrochimica Acta 2005;50:1189–96. https://doi.org/10.1016/j.electacta.2004.07.044.
[70] Maksimović VM, Lačnjevac UČ, Stoiljković MM, Pavlović MG, Jović VD. Morphology and composition of Ni–Co electrodeposited powders. Materials Characterization 2011;62:1173–9. https://doi.org/10.1016/j.matchar.2011.09.001.
[71] Lu W, Liebscher CH, Dehm G, Raabe D, Li Z. Bidirectional Transformation Enables Hierarchical Nanolaminate Dual-Phase High-Entropy Alloys. Adv Mater 2018;30:1804727. https://doi.org/10.1002/adma.201804727.
[72] Lian K, Thorpe SJ, Kirk DW. The electrocatalytic activity of amorphous and crystalline Ni□Co alloys on the oxygen evolution reaction. Electrochimica Acta 1992;37:169–75. https://doi.org/10.1016/0013-4686(92)80026-I.
[73] Lian KK. Hydrous Oxide Film Growth on Amorphous Ni-Co Alloys. J Electrochem Soc 1991;138:2877. https://doi.org/10.1149/1.2085333.
[74] Pérez-Alonso FJ, Adán C, Rojas S, Peña MA, Fierro JLG. Ni–Co electrodes prepared by electroless-plating deposition. A study of their electrocatalytic activity for the hydrogen and oxygen evolution reactions. International Journal of Hydrogen Energy 2015;40:51–61. https://doi.org/10.1016/j.ijhydene.2014.11.015.
[75] Anantharaj S, Ede SR, Karthick K, Sam Sankar S, Sangeetha K, Karthik PE, et al. Precision and correctness in the evaluation of electrocatalytic water splitting: revisiting

activity parameters with a critical assessment. Energy Environ Sci 2018;11:744–71. https://doi.org/10.1039/C7EE03457A.
[76] Zeng K, Zhang D. Recent progress in alkaline water electrolysis for hydrogen production and applications. Progress in Energy and Combustion Science 2010;36:307–26. https://doi.org/10.1016/j.pecs.2009.11.002.
[77] Darband GB, Aliofkhazraei M, Shanmugam S. Recent advances in methods and technologies for enhancing bubble detachment during electrochemical water splitting. Renewable and Sustainable Energy Reviews 2019;114:109300. https://doi.org/10.1016/j.rser.2019.109300.
[78] Wen R, Xu S, Ma X, Lee Y-C, Yang R. Three-Dimensional Superhydrophobic Nanowire Networks for Enhancing Condensation Heat Transfer. Joule 2018;2:269–79. https://doi.org/10.1016/j.joule.2017.11.010.
[79] Ahn SH, Choi I, Park H-Y, Hwang SJ, Yoo SJ, Cho E, et al. Effect of morphology of electrodeposited Ni catalysts on the behavior of bubbles generated during the oxygen evolution reaction in alkaline water electrolysis. Chem Commun 2013;49:9323. https://doi.org/10.1039/c3cc44891f.
[80] Grubač Z, Sesar A. Electrocatalytic Activity of the Ni57.3Co42.7 Alloy for the Hydrogen Evolution. Croat Chem Acta 2017;90. https://doi.org/10.5562/cca3174.
[81] Santos DMF, Amaral L, Šljukić B, Macciò D, Saccone A, Sequeira CAC. Electrocatalytic Activity of Nickel-Cerium Alloys for Hydrogen Evolution in Alkaline Water Electrolysis. J Electrochem Soc 2014;161:F386–90. https://doi.org/10.1149/2.016404jes.
[82] Tian T, Huang L, Ai L, Jiang J. Surface anion-rich NiS_2 hollow microspheres derived from metal–organic frameworks as a robust electrocatalyst for the hydrogen evolution reaction. J Mater Chem A 2017;5:20985–92. https://doi.org/10.1039/C7TA06671F.
[83] Herraiz-Cardona I, Ortega E, Antón JG, Pérez-Herranz V. Assessment of the roughness factor effect and the intrinsic catalytic activity for hydrogen evolution reaction on Ni-based electrodeposits. International Journal of Hydrogen Energy 2011;36:9428–38. https://doi.org/10.1016/j.ijhydene.2011.05.047.
[84] Pi M, Wu T, Guo W, Wang X, Zhang D, Wang S, et al. Phase-controlled synthesis of polymorphic tungsten diphosphide with hybridization of monoclinic and orthorhombic phases as a novel electrocatalyst for efficient hydrogen evolution. Journal of Power Sources 2017;349:138–43. https://doi.org/10.1016/j.jpowsour.2017.03.040.
[85] Zhang Y, Wang Y, Han C, Jia S, Zhou S, Zang J. Tungsten-coated nano-boron carbide as a non-noble metal bifunctional electrocatalyst for oxygen evolution and hydrogen evolution reactions in alkaline media. Nanoscale 2017;9:19176–82. https://doi.org/10.1039/C7NR08092A.
[86] Jiao M, Chen Z, Zhang X, Mou K, Liu L. Multicomponent N doped graphene coating Co@Zn heterostructures electrocatalysts as high efficiency HER electrocatalyst in alkaline electrolyte. International Journal of Hydrogen Energy 2020;45:16326–36. https://doi.org/10.1016/j.ijhydene.2020.04.121.
[87] Zhang C, Bhoyate S, Kahol PK, Siam K, Poudel TP, Mishra SR, et al. Highly Efficient and Durable Electrocatalyst Based on Nanowires of Cobalt Sulfide for Overall Water Splitting. ChemNanoMat 2018;4:1240–6. https://doi.org/10.1002/cnma.201800301.
[88] Shit S, Chhetri S, Jang W, Murmu NC, Koo H, Samanta P, et al. Cobalt Sulfide/Nickel Sulfide Heterostructure Directly Grown on Nickel Foam: An Efficient and Durable Electrocatalyst for Overall Water Splitting Application. ACS Appl Mater Interfaces 2018;10:27712–22. https://doi.org/10.1021/acsami.8b04223.
[89] Zhang Q, Ye C, Li XL, Deng YH, Tao BX, Xiao W, et al. Self-Interconnected Porous Networks of NiCo Disulfide as Efficient Bifunctional Electrocatalysts for Overall Water

Splitting. ACS Appl Mater Interfaces 2018;10:27723–33. https://doi.org/10.1021/acsami.8b04386.
[90] Zhao T, Gao J, Wu J, He P, Li Y, Yao J. Highly Active Cobalt/Tungsten Carbide@N- Doped Porous Carbon Nanomaterials Derived from Metal- Organic Frameworks as Bifunctional Catalysts for Overall Water Splitting. Energy Technol 2019;7:1800969. https://doi.org/10.1002/ente.201800969.
[91] Goranova D, Lefterova E, Rashkov R. Electrocatalytic activity of Ni-Mo-Cu and Ni-Co-Cu alloys for hydrogen evolution reaction in alkaline medium. International Journal of Hydrogen Energy 2017;42:28777–85. https://doi.org/10.1016/j.ijhydene.2017.10.002.

Supplementary Material

Click here to download Supplementary Material: Supplementary Material_rev.pdf

***Declaration of Interest Statement**

Declaration of interests

☒ The authors declare that they have no known competing financial interests or personal relationships that could have appeared to influence the work reported in this paper.

☐The authors declare the following financial interests/personal relationships which may be considered as potential competing interests: